

Vapor–Liquid–Solid Phase Transitions in Aqueous Sodium Sulfate and Sodium Carbonate from Heat Capacity Measurements near the First Critical End Point. 1. Sodium Sulfate

Ilmutdin M. Abdulagatov,^{*,†,‡} Boris A. Mursalov,[†] and Vasilii I. Dvoryanchikov[†]

Institute for Geothermal Problems of the Dagestan Scientific Center of the Russian Academy of Sciences, 367030 Makhachkala, Shamilya 39 A, Dagestan, Russia

Heat capacities at constant volume and composition are reported for aqueous sodium sulfate for three compositions, 1 mass %, 5 mass %, and 10 mass %, respectively, and along 19 isochores, from 250 kg·m⁻³ to 1073 kg·m⁻³ in the temperature range from 350 K to 670 K. In the range from 630 K to 650 K, many of these isochores display two features in the heat capacity as a function of the temperature: one peak or step when solid salt first precipitates and, on further heating, a λ -shaped peak when the vapor- or liquid-phase disappears. In Part 2 of this paper, these features will be interpreted.

Introduction

There has been growing interest in aqueous solutions at near-critical and supercritical conditions due to their importance in supercritical water oxidation (SCWO) technology. SCWO technology is an emerging technology for the destruction of civilian and military hazardous wastes. One of the important applications of SCWO for waste treatment is in the handling of solids which can be present at high temperatures and high pressures. Sodium sulfate is one of the most commonly encountered salts in prospective applications of SCWO. Development of effective strategies for applying SCWO technology to the destruction of hazardous materials requires knowledge of the thermodynamic properties of aqueous salt solutions near the critical point. This paper presents new isochoric heat capacity data for aqueous sodium sulfate at temperatures up to 670 K. Sodium sulfate, or Glauber salt, was a mainstay of the German chemical and pharmaceutical industry in the 19th century. The salt has a complex phase diagram. Above 250 °C, however, in the range of declining solubility of interest here, the solid salt exists in dehydrated form only. The solid phase extends above the critical point of water; thus, cutting off the saltwater critical line in a critical end point. This so-called Type-2 solid–liquid–vapor phase behavior, typical for sodium sulfate, sodium carbonate (Abdulagatov et al.¹), and many other salts poorly soluble in water, will be described in more detail in Valyashko et al.,² Part 2 of this series.

Interest in sodium sulfate was reactivated recently because the salt is formed, and found to clog the reactor tubes, during the process of SCWO of sulfur-containing organic waste, when caustic is added for neutralization. Armellini and Tester³ (MIT) studied the kinetics of salt deposition under near-critical conditions. Salt deposition from aqueous sodium sulfate was studied in a collaboration.^{3,4}

At the Dagestan Scientific Center of the Russian Academy of Sciences, the heat capacity $C_{v,x}$ of aqueous sodium

Table 1. Typical Ramp Rates for Some Isochores at Density ρ

$\rho/\text{kg}\cdot\text{m}^{-3}$	rate/ $\text{K}\cdot\text{s}^{-1}$ (heating and cooling)
697.8	from 6.07×10^{-4} to 7.55×10^{-4}
537.6	from 7.15×10^{-4} to 8.97×10^{-4}
537.6	from 5.77×10^{-4} to 7.27×10^{-4}
490.0	from 3.45×10^{-4} to 11.79×10^{-4}

sulfate has been measured in two or three coexisting phases at constant overall volume V and mass fraction x . Although some of the results have appeared in print before (Abdulagatov et al.⁵), the comprehensive set of 19 isochores at three compositions is included here for the first time. Many of these isochores show two characteristic features. In a heating run, first a step or peak appears when solid salt begins to drop out of solution. Some runs were taken both in the heating and the cooling mode. At a higher temperature, either the liquid or the vapor phase disappears, with a characteristic λ -shaped peak for those isochores that are close to the critical density for the solution. In the present paper, the data are presented. In a follow-up paper, Valyashko et al.,² Part 2 in this series, an interpretation is given of the features in the data, and a comparison is made with data from the literature.

Experimental Section

Measurements of the isochoric heat capacity of sodium sulfate and sodium carbonate solutions were made in a spherical high-temperature, high-pressure adiabatic calorimeter, of a design pioneered by Amirkhanov et al.⁶ The present calorimeter has been described in a recent paper in this journal (Abdulagatov et al.⁷), and additional detail is given by Mursalov et al.⁸ The spherical vessel is constructed of heat- and corrosion-resistant 1X18H9T stainless steel and has a volume of 101.45 cm³. The contents of the vessel are stirred prior to measurement. Heat capacities are measured in a ramping heating mode; occasionally, a cooling mode is used. The ramp rate is varied, to make sure that the heat capacity does not depend on the ramp rate. Some typical optimal ramp rates are given in Table 1. The papers by Abdulagatov et al.⁷ and Mursalov et al.⁸ contain a detailed analysis of all sources of uncertainty likely to affect the determination of $C_{v,x}$ with

* To whom correspondence should be addressed.

[†] Institute for Geothermal Problems of the Dagestan Scientific Center of the Russian Academy of Sciences. E-mail: mangur@datacom.ru.

[‡] Present address: National Institute of Standards and Technology, Boulder, CO 80303. E-mail: ilmutdin@boulder.nist.gov.

Table 2. Experimental Values of the Heat Capacities C_{vx} along Isochores in Aqueous Sodium Sulfate

T K	C_{vx} kJ·kg ⁻¹ ·K ⁻¹	T K	C_{vx} kJ·kg ⁻¹ ·K ⁻¹	T K	C_{vx} kJ·kg ⁻¹ ·K ⁻¹
1 mass % Na ₂ SO ₄ $\rho = 250.1 \text{ kg}\cdot\text{m}^{-3}$					
585.29	6.231	630.22	10.294	647.78	6.079
585.46	6.759	631.24	10.340	647.95	5.972
585.64	6.650	631.41	10.341	648.12	4.473
585.82	6.667	631.59	10.237	648.29	4.485
585.98	6.443	646.41	13.323	648.63	4.042
629.02	8.972	646.58	13.577	648.80	4.119
629.19	8.868	646.75	13.705	648.97	4.120
629.38	8.963	646.92	13.620	649.31	4.054
629.54	8.867	647.08	13.520	665.65	3.410
629.68	13.406	647.26	10.300	665.82	3.275
629.87	10.350	647.43	9.033	665.99	3.276
630.05	10.297	647.60	7.135		
$\rho = 309.9 \text{ kg}\cdot\text{m}^{-3}$					
588.44	5.528	631.76	8.089	647.78	16.085
588.61	5.560	631.93	8.509	647.95	16.073
588.79	5.753	632.10	12.225	648.12	6.255
588.96	5.772	632.27	9.270	648.29	5.577
589.14	5.775	632.44	9.228	648.46	5.235
630.56	8.024	632.61	9.280	648.63	5.144
630.73	8.086	632.78	9.275	648.80	4.972
630.90	8.021	647.02	13.437	648.97	5.086
631.24	8.012	647.26	14.043	649.14	5.257
631.41	8.017	647.43	14.638	649.31	5.173
631.59	8.012	647.60	15.235	649.48	5.085
$\rho = 361.9 \text{ kg}\cdot\text{m}^{-3}$					
583.71	5.502	633.29	8.935	649.65	4.569
583.88	5.331	633.46	9.088	649.82	4.570
584.06	5.331	633.73	9.088	649.99	4.570
584.23	5.333	634.66	9.195	650.16	4.595
584.41	5.332	634.83	9.125	652.71	4.049
624.75	7.397	635.00	9.110	652.88	4.049
624.92	7.383	635.17	9.253	653.05	4.031
625.09	7.417	635.34	9.254	653.22	4.061
625.26	7.327	635.51	9.340	653.39	4.061
625.43	7.322	646.92	12.520	653.56	3.964
631.07	7.891	647.09	12.829	653.73	4.052
631.14	7.887	647.26	14.084	653.89	3.966
631.41	7.799	647.43	13.983	654.06	4.096
631.59	7.885	647.60	15.345	654.23	4.097
631.76	7.881	647.78	16.178	667.01	3.337
631.93	7.848	647.95	8.749	667.18	3.340
632.10	7.902	648.12	5.817	667.35	3.253
632.27	7.881	648.29	5.353	667.52	3.328
632.44	7.830	648.46	5.177	667.69	3.298
632.61	7.825	648.63	4.779	667.86	3.124
632.78	7.907	649.14	4.737	668.32	3.327
632.95	11.473	649.31	4.740	668.55	3.251
633.12	9.464	649.48	4.743		
$\rho = 521.3 \text{ kg}\cdot\text{m}^{-3}$					
630.05	6.394	634.83 ^{C_a}	7.422	636.02	8.077
630.22	6.521	634.83	6.872	637.39	7.852
630.39	6.447	635.00	6.757	637.56	7.851
630.56	6.540	635.00 ^C	7.613	637.73	7.912
630.73	6.344	635.17 ^C	7.675	637.90	7.813
632.95	6.400	635.17	9.003	638.07	7.807
633.12	6.396	635.34	9.184	638.41	3.170
633.29	6.399	635.34 ^C	7.734	638.58	3.108
633.46	6.403	635.51 ^C	7.735	639.75	3.111
634.15 ^C	6.740	635.51	8.095	639.92	3.106
634.32 ^C	7.067	635.68	8.019	662.75	2.927
634.49 ^C	7.305	635.68 ^C	7.857	662.92	2.954
634.49	6.797	635.85 ^C	7.908	663.09	2.906
634.66	6.741	635.85	8.070	663.26	2.931
634.66 ^C	7.307				
$\rho = 664.0 \text{ kg}\cdot\text{m}^{-3}$					
591.24	5.024	599.94	5.280	602.19	2.999
591.41	4.974	600.11	5.175	602.37	3.020
591.58	5.046	600.46	3.036	602.54	3.000
591.76	5.025	600.63	2.798	602.71	3.019
592.93	5.025	600.81	2.846	610.49	2.956
593.10	4.980	600.98	2.846	610.66	2.977
599.42	5.261	601.15	2.977	610.83	2.976
599.59	5.217	601.33	2.992	611.01	2.978
599.77	5.221	602.02	2.999	611.18	2.978

Table 2. (continued)

T	C_{vx}	T	C_{vx}	T	C_{vx}
K	$\text{kJ} \cdot \text{kg}^{-1} \cdot \text{K}^{-1}$	K	$\text{kJ} \cdot \text{kg}^{-1} \cdot \text{K}^{-1}$	K	$\text{kJ} \cdot \text{kg}^{-1} \cdot \text{K}^{-1}$
1 mass % Na_2SO_4					
$\rho = 860.5 \text{ kg} \cdot \text{m}^{-3}$					
492.17	4.457	493.51	3.364	494.84	3.185
492.36	4.432	493.70	3.311	513.32	3.279
492.55	4.408	493.89	3.234	513.52	3.234
492.74	4.495	494.08	3.180	513.70	3.236
492.93	4.451	494.27	3.312	513.88	3.283
493.13	3.586	494.46	3.188	514.07	3.261
493.32	3.630	494.65	3.234	514.26	3.304
5 mass % Na_2SO_4					
$\rho = 490.0 \text{ kg} \cdot \text{m}^{-3}$					
608.93	5.143	643.35	8.829	644.71	3.476
609.11	5.168	643.52	8.913	644.72 ^C	3.386
609.28	5.068	643.69	8.687	644.80 ^C	3.449
609.45	5.080	643.86	8.996	644.88	3.199
609.63	5.091	644.03	8.719	644.89 ^C	3.509
609.97	12.519	644.11 ^C	7.687	645.05	3.145
610.14	6.613	644.20 ^C	8.074	645.17	3.199
610.32	6.565	644.20	7.507	645.39	3.199
610.49	6.517	644.29 ^C	9.129	645.56	3.145
637.37	7.961	644.37	6.607	647.09	3.208
637.54	7.810	644.38 ^C	3.581	647.26	3.292
637.71	7.980	644.46 ^C	3.506	647.43	3.292
638.23	7.962	644.54	3.201	647.60	3.248
643.01	8.567	644.55 ^C	3.377	647.77	3.173
643.18	8.633	644.63 ^C	3.386		
$\rho = 674.7 \text{ kg} \cdot \text{m}^{-3}$					
607.56	4.682	611.01	6.468	616.17	2.873
607.73	4.828	611.18	6.419	616.69	2.871
607.90	4.643	611.52	6.397	616.86	2.814
608.07	4.627	611.87	6.352	617.54	2.754
608.94	4.850	612.04	6.400	617.72	2.749
609.80	4.851	612.21	6.342	631.93	3.049
609.97	4.854	615.31	6.565	632.10	3.050
610.32	4.798	615.48	6.679	632.44	2.979
610.49	4.790	615.65	6.504	632.61	3.015
610.66	11.605	616.00	2.836		
$\rho = 925.9 \text{ kg} \cdot \text{m}^{-3}$					
460.35	3.383	461.53	3.049	480.57	2.711
460.55	3.352	461.73	2.802	480.77	2.760
460.74	3.409	462.12	2.821	480.96	2.645
460.94	3.268	462.32	2.727	481.16	2.718
461.14	2.793	462.52	2.610	481.36	2.743
461.34	2.853	462.72	2.798		
10 mass % Na_2SO_4					
$\rho = 537.6 \text{ kg} \cdot \text{m}^{-3}$					
590.54 ^C	4.371	592.46	9.639	641.30	7.865
590.71 ^C	4.368	592.46 ^C	5.660	641.48	8.012
590.89 ^C	4.370	592.63 ^C	5.602	641.65	8.166
591.06 ^C	4.337	592.63	6.466	641.82	8.477
591.41 ^C	4.335	592.81 ^C	5.735	641.99	8.318
591.58 ^C	5.383	592.98 ^C	5.686	642.16	8.315
591.58	4.441	593.33	5.968	642.33	8.313
591.76	4.366	593.50	6.050	642.50	8.155
591.76 ^C	5.264	593.68	5.930	642.67	7.907
591.93 ^C	5.441	593.85	6.123	642.84	7.482
591.93	4.484	594.03	6.178	643.18	2.978
592.11	4.428	640.55	7.631	643.35	2.978
592.11 ^C	5.520	640.62	7.882	643.52	2.976
592.28 ^C	5.570	640.79	7.885	643.69	2.951
592.28	5.146	640.96	7.855		
$\rho = 697.8 \text{ kg} \cdot \text{m}^{-3}$					
591.24 ^C	4.765	593.15 ^C	5.570	619.26	6.385
591.41 ^C	4.744	593.33 ^C	5.454	619.43	6.119
591.58 ^C	4.862	593.50 ^C	5.981	619.60	3.422
591.76 ^C	4.884	593.68	5.732	619.78	2.692
591.93	4.411	593.68 ^C	5.546	619.95	2.690
591.93 ^C	4.883	593.85 ^C	5.837	620.12	2.642
592.11 ^C	5.072	594.20	5.841	631.59	2.717
592.11	4.430	594.37	5.912	631.76	2.763
592.28	4.393	594.55	5.868	631.93	2.716
592.28 ^C	5.560	594.72	5.954	632.10	2.835
592.46	4.406	594.90	5.933	632.27	2.726
592.46 ^C	5.592	618.58	6.517	632.78	2.751
592.63 ^C	5.643	618.75	6.486	640.45	2.721
592.81	4.367	618.92	6.503	640.62	2.671
592.81 ^C	5.589	619.09	6.428	640.79	2.670
592.98 ^C	5.591				

Table 2. (continued)

T	C_{vx}	T	C_{vx}	T	C_{vx}
K	$\text{kJ} \cdot \text{kg}^{-1} \cdot \text{K}^{-1}$	K	$\text{kJ} \cdot \text{kg}^{-1} \cdot \text{K}^{-1}$	K	$\text{kJ} \cdot \text{kg}^{-1} \cdot \text{K}^{-1}$
10 mass % Na_2SO_4					
$\rho = 774.2 \text{ kg} \cdot \text{m}^{-3}$					
589.66	4.398	592.94 ^C	5.324	602.71	6.032
589.84	4.399	592.98	4.403	602.89	6.027
590.01	4.381	593.03	4.396	603.06	6.025
590.19	4.397	593.15	4.398	603.23	5.979
591.58 ^C	4.188	593.33	4.402	603.41	5.984
591.76 ^C	4.117	593.33 ^C	5.407	603.58	3.565
591.93 ^C	4.226	593.50 ^C	5.402	603.75	2.497
591.93	4.395	593.50	4.400	603.93	2.440
592.11	4.396	593.68	4.405	604.10	2.557
592.11 ^C	4.262	593.68 ^C	5.544	604.27	2.439
592.28 ^C	4.404	593.85 ^C	5.535	604.46	2.678
592.46 ^C	4.833	593.85	13.420	604.62	2.678
592.46	4.395	594.03 ^C	5.550	604.79	2.681
592.63 ^C	5.116	594.20 ^C	5.554	604.96	2.681
592.81 ^C	5.259	594.20	5.982	605.14	2.678
592.81	4.327	602.54	6.053		
$\rho = 796.2 \text{ kg} \cdot \text{m}^{-3}$					
476.59	3.636	589.14	4.383	596.64	5.930
476.78	3.643	589.31	4.381	596.81	5.935
476.98	3.642	589.49	4.402	597.16	5.996
477.17	3.627	589.84	4.350	597.85	5.875
477.36	3.660	590.36	4.393	598.03	5.787
477.56	3.661	590.71	4.353	598.38	6.024
477.95	3.632	590.89	4.340	598.72	2.734
478.14	3.658	591.06	4.353	598.90	2.733
478.33	3.693	593.85	5.652	599.42	2.729
478.53	3.663	594.03	5.690	613.25	2.697
574.90	4.244	594.20	5.697	613.42	2.697
575.07	4.157	594.55	5.839	613.59	2.738
575.25	4.199	595.42	5.858	613.77	2.697
575.78	4.237	595.59	5.900		
$\rho = 830.7 \text{ kg} \cdot \text{m}^{-3}$					
587.21	4.402	590.01	2.625	606.52	2.791
587.38	4.267	590.19	2.736	606.70	2.639
587.56	4.265	590.36	2.687	607.04	2.746
587.73	4.213	590.53	2.688	607.21	2.746
587.91	3.035	590.71	2.686	607.39	2.599
588.09	2.782	590.89	2.735	607.56	2.701
588.26	2.731	591.06	2.684	607.91	2.647
588.44	2.832	591.24	2.735	608.08	2.728
588.96	2.731	605.83	2.739	608.25	2.674
589.14	2.683	606.00	2.688	608.42	2.667
589.31	2.685	606.18	2.791	608.60	2.662
589.49	2.736	606.35	2.688	608.77	2.672
589.83	2.625				
$\rho = 844.8 \text{ kg} \cdot \text{m}^{-3}$					
476.81	3.952	528.54	4.088	580.54	2.665
476.01	3.958	578.60	4.346	580.72	2.638
476.20	3.953	578.78	4.344	581.07	2.657
476.39	3.953	579.13	4.323	581.42	2.666
476.59	3.977	579.31	4.351	597.33	2.557
476.98	3.941	579.66	4.330	597.82	2.583
527.80	4.042	579.75	2.640	598.03	2.568
527.98	4.000	579.84	2.702	598.20	2.589
528.17	3.947	580.01	2.696		
$\rho = 936.3 \text{ kg} \cdot \text{m}^{-3}$					
514.82	4.006	516.50	3.974	518.36	2.905
515.00	4.023	516.68	2.891	534.42	2.840
515.19	3.997	516.87	2.860	534.45	2.827
515.37	4.020	517.05	2.879	534.97	2.829
515.56	3.985	517.24	2.880	535.15	2.791
515.94	3.960	517.98	2.888	535.33	2.816
516.12	3.972	518.17	2.874		
$\rho = 989.2 \text{ kg} \cdot \text{m}^{-3}$					
467.62	3.968	468.99	3.954	478.33	2.716
467.82	3.984	469.38	3.001	478.53	2.996
468.02	4.007	469.58	3.007	488.15	2.960
468.21	4.000	469.67	2.985	488.35	2.994
468.41	3.944	477.65	2.977	488.73	2.995
468.60	3.964	477.95	3.014	488.92	2.953
468.80	3.917	478.14	2.978		

Table 2. (continued)

T K	C_{vx} kJ·kg ⁻¹ ·K ⁻¹	T K	C_{vx} kJ·kg ⁻¹ ·K ⁻¹	T K	C_{vx} kJ·kg ⁻¹ ·K ⁻¹
10 mass % Na ₂ SO ₄					
$\rho = 774.2 \text{ kg}\cdot\text{m}^{-3}$					
$\rho = 1059.0 \text{ kg}\cdot\text{m}^{-3}$					
383.06	3.768	384.37	3.716	385.67	3.380
383.28	3.796	384.58	3.528	385.89	3.372
383.50	3.823	384.80	3.476	385.27	3.366
383.71	3.821	385.02	3.395	385.48	3.362
383.93	3.743	385.24	3.367	385.70	3.379
384.15	3.746	385.45	3.363	385.92	3.371
$\rho = 1072.5 \text{ kg}\cdot\text{m}^{-3}$					
352.56	3.887	353.93	3.867	355.54	3.554
352.79	3.890	354.16	3.885	356.22	3.527
353.02	3.905	354.39	3.594	356.45	3.536
353.25	3.909	354.85	3.568	356.67	3.572
353.47	3.859	355.08	3.550	357.13	3.517
353.70	3.877	355.30	3.539		

^a Values of isochoric heat capacities obtained on cooling are indicated by a superscript C.

allowance for the propagation of uncertainty from temperature and heat measurement, as well as from not strictly isochoric conditions of the process. The uncertainty in C_{vx} measurements arises from two general types of uncertainties: measurement uncertainties and nonmeasurement uncertainties. Measurement uncertainties were associated with uncertainties that exist in the measured quantities (m , ΔQ , ΔT , and C_0) contained in the working equation

$$C_v = \frac{1}{m} \left\{ \frac{\Delta Q}{\Delta T} - C_0 \right\} \quad (1)$$

where m is the mass of the sample in the calorimeter, ΔQ is the amount of heat released by the internal heater, C_0 is the heat capacity of the empty calorimeter, and ΔT is the temperature change resulting from the addition of an amount of heat ΔQ . Nonmeasurement uncertainties were associated with deviations of actual experimental conditions from the mathematical model used to derive the equation for computing the heat capacity. The relative uncertainties in measured quantities are $\delta(\Delta Q) = 0.08\%$, $\delta(\Delta T) = (0.02 \text{ to } 0.05) \text{ K}$ depending on the magnitude of ΔT , $\delta m = 0.01\%$, and $\delta(C_0) = (0.5 \text{ to } 1.5)\%$ depending on the temperature range. The temperature was determined with an uncertainty not exceeding 10 mK. The major sources of nonmeasurement uncertainties are: (1) the non-isochoric behavior of the apparatus (deviations of the system from a constant volume) during heating, (2) the non-adiabatic conditions of the system, and (3) stray heat flows through the calorimeter not controlled by the semiconductor layer, for example, parasitic flows caused by spurious temperature differences. The correction related to the non-isochoric behavior during heating is about 0.5 to 1.0% of the total magnitude of the heat capacity. The possible supply or removal of heat through the layer of the thermoelement caused by the imperfect adiabatic behavior of the calorimetric system was estimated from the relation

$$\Delta Q = \lambda \frac{\Delta T}{d} S \tau \quad (2)$$

where $\lambda \approx 2.09 \text{ W}\cdot\text{m}^{-1}\cdot\text{K}^{-1}$ is the thermal conductivity of the semiconductor layer (cuprous oxide), S is the surface area of the cuprous oxide layer, d is the thickness of the cuprous oxide layer, and $\Delta T \approx 10^{-4} \text{ K}$ is the temperature difference between inner and outer calorimetric vessels. The average time of one measurement was $\tau = 300 \text{ s}$, and

the heat losses ΔQ for this time were 0.2 J or 0.02% of the total heat supplied to the system. The heat losses through the areas of the calorimeter that are not controlled by the thermoelement (the well for the internal heater or the resistance thermometer) do not exceed $4 \times 10^{-4} \text{ J}$. The heat loss through the capillary used to fill the calorimeter with the sample is 0.003 J. Heat losses through the inlet and outlet wires of the internal heater were 0.066 J, and those through the wires of the temperature sensor were 0.0016 J. The heat flow through all uncontrolled areas was 0.27 J or 0.06% of the total amount of heat supplied to the system. On the basis of detailed analysis, all sources of uncertainties likely to affect the determination of C_v were 1 to 1.5% in the liquid phase, 2 to 3% in the vapor phase, and 4 to 5% near the critical point. The uncertainty of the phase transition temperature measurements is about 0.01 to 0.02 K.

All original temperature data, as well as the experimental C_{vx} data themselves, have been corrected for conversion from IPTS-68 to ITS-90 temperature scales (Rusby⁹). At temperatures below 400 K the correction of C_{vx} is only 0.0008%, orders of magnitude below the experimental uncertainty. For temperatures approaching 670 K, the C_{vx} correction reached up to 0.027%, still well below the experimental uncertainty.

Heat capacity data for aqueous sodium sulfate were obtained for three compositions, 1 mass %, 5 mass %, and 10 mass %, respectively, and along 19 isochores from 250 kg·m⁻³ to 1073 kg·m⁻³, in the temperature range from 350 K to 670 K. The data are listed in Table 2. The column heading lists the average density of the isochore, which are equal to the mass of solution divided by the volume of the calorimeter at ambient conditions. Most data were obtained in a heating ramping mode. Those obtained in a cooling ramping mode are marked with a superscript C in Table 2. The data for sodium carbonate, which will be referred to in Part 2 of this series, were published in Abdulagatov et al.¹

Phase Transitions on Isochoric Heating

Plots of some typical isochores are shown in Figure 1. It is clear that several effects are taking place when the sodium sulfate solution is heated isochorically. Two peaks or jumps are often found. The first peak or jump, at the lower temperature, is associated with the appearance of the solid phase. The second peak or jump accompanies the

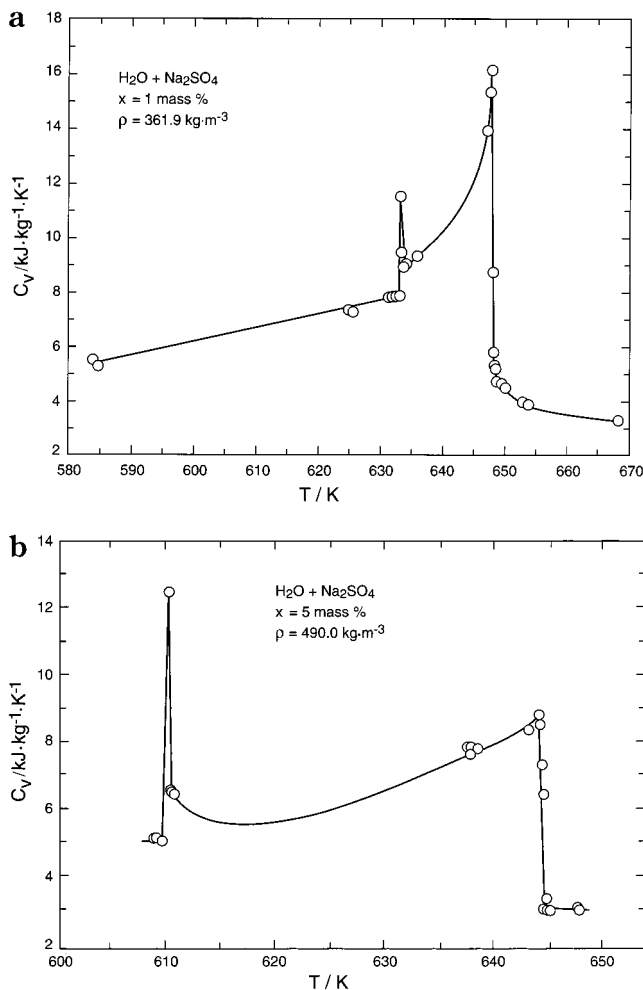


Figure 1. (a and b) Typical $C_{v,x}$ behavior as a function of temperature along isochores for two choices of overall concentration and density.

disappearance of the vapor or liquid phase. The phase behavior will be fully explored and explained, and the phase boundaries delineated, in Valyashko et al.,² Part 2 of this series.

Conclusions

A set of constant-volume, constant-overall-composition heat capacity data for aqueous Na₂SO₄ solutions is pre-

sented. The data extend over a sizable range in density and temperature around the critical point of water. The isochoric heat capacity as a function of temperature may show one or two jumps or spikes, which are indicative of the appearance or disappearance of solid or fluid phases, as explained by Valyashko et al.,² Part 2 of this series.

Literature Cited

- (1) Abdulagatov, I. M.; Dvoryanchikov, V. I.; Mursalov, B. A.; Kamalov, A. N. Heat capacity at constant volume of H₂O + Na₂CO₃ solutions near the critical point of pure water. *J. Solution Chem.* **1999**, *28*, 871–889.
- (2) Valyashko, V. M.; Abdulagatov, I. M.; Levelt Sengers, J. M. H. Vapor–Liquid–Solid Phase Transitions in Aqueous Sodium Sulfate and Sodium Carbonate from Heat Capacity Measurements near the First Critical End Point. 2. Phase Boundaries. *J. Chem. Eng. Data* **2000**, *45*, 1139.
- (3) Armellini, F. J.; Tester, J. W. Precipitation of sodium chloride and sodium sulfate in water from sub- to supercritical conditions: 150 to 550 °C, 100 to 300 bar. *J. Supercrit. Fluids* **1994**, *7*, 147–158.
- (4) Hodes, M. S.; Smith, K. A.; Hurst, W. S.; Bowers, W. J., Jr.; Griffith, P.; Sako, K. Measurements and analysis of solubilities and deposition rates in near-supercritical, aqueous, sodium sulfate and potassium sulfate solutions. In preparation for *J. Supercrit. Fluids*.
- (5) Abdulagatov, I. M.; Dvoryanchikov, V. I.; Mursalov, B. A.; Kamalov, A. N. Measurements of the heat capacity at constant volume of H₂O + Na₂SO₄ in near-critical and supercritical water. *Fluid Phase Equilib.* **1998**, *150*, 525–535.
- (6) Amirkhanov, Kh. I.; Stepanov, G. V.; Alibekov, B. G. *Isochoric Heat Capacity of Water and Steam*; Amerind Publ. Co.: New Delhi, 1974.
- (7) Abdulagatov, I. M.; Dvoryanchikov, V. I.; Kamalov, A. N. Heat capacity at constant volume of pure water in the temperature range 412–693 K at densities from 250 to 925 kg m⁻³. *J. Chem. Eng. Data* **1998**, *43*, 830–838.
- (8) Mursalov, B. A.; Abdulagatov, I. M.; Dvoryanchikov, V. I.; Kamalov, A. N.; Kiselev, S. B. Isochoric heat capacity of heavy water at subcritical and supercritical conditions. *Int. J. Thermophys.* **1999**, *20*, 1497–1528.
- (9) Rusby, R. L. The conversion of thermal reference values to the ITS-90. *J. Chem. Thermodyn.* **1991**, *23*, 1153–1161.

Acknowledgment

I.M.A. acknowledges the hospitality of the Division of Physical and Chemical Properties at NIST and the advice and encouragement of Dr. J. Magee.

Received for review April 27, 2000. Accepted August 22, 2000. The experimental work was supported by INTAS Grant No. INTAS-96-1989.

JE0001227